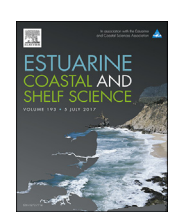


Contents lists available at ScienceDirect

# Estuarine, Coastal and Shelf Science

journal homepage: www.elsevier.com/locate/ecss



# The effect of evaporation on the erodibility of mudflats in a mesotidal estuary



S. Fagherazzi <sup>a, \*</sup>, T. Viggato <sup>a</sup>, A.M. Vieillard <sup>a</sup>, G. Mariotti <sup>c</sup>, R.W. Fulweiler <sup>a, b</sup>

- <sup>a</sup> Department of Earth and Environment, Boston University, Boston, MA, USA
- <sup>b</sup> Department of Biology, Boston University, Boston, MA, USA
- <sup>c</sup> Department of Oceanography and Coastal Sciences, Louisiana State University, Baton Rouge, LA, USA

#### ARTICLE INFO

Article history: Received 4 April 2017 Received in revised form 6 June 2017 Accepted 8 June 2017 Available online 9 June 2017

#### ABSTRACT

Large areas of mesotidal estuaries become subaerial during low tide. Here we study the effect of several meteorological and hydrodynamic parameters on the erodibility of mudflat substrates when they are subaerial. Field measurements carried out over a two-week period in September 2011 in Plum Island Sound, Massachusetts USA, indicate that high evaporation rates and long subaerial periods are associated to low sediment erodibility. Sediment concentrations in the water column during submergence depend on bottom shear stresses triggered by tidal currents. Surprisingly, they are also related to the total evaporation that occurred in the previous emergence period. We conclude that low erodibility of mudflat sediments is linked to subaerial desiccation at low tide. This strengthening effect is not lost during the following submerged period, thus limiting the erosive effect of tidal currents. We thus show that not only subaqueous but also subaerial processes might control the erodibility of mudflats. Long-term evaporation rates can therefore directly affect the stability of mudflats in mesotidal environments.

© 2017 Elsevier Ltd. All rights reserved.

### 1. Introduction

Mudflats are an important component of the coastal landscape: they protect coastal communities from flooding and storm surges (Scavia et al., 2002; Meire et al., 2005), maintain water quality through nutrient cycling and pollutant filtration (Van Damme et al., 2005), and provide a critical foraging habitat for birds and fish (Little, 2000; Galbraith et al., 2002).

Meteorological and tidal conditions affect sediment erosion and deposition in mudflats, the geotechnical properties of the substrate, as well as their biological variability and productivity (Amos et al., 1988). Anthropogenic stressors such as coastal nutrient pollution and climate change have the potential to alter the biological and physical equilibrium of mudflats (Galbraith et al., 2002; Meire et al., 2005). For example, an increase in the frequency of storms combined with sea level rise could significantly alter erosion rates and the overall morphology of tidal flats (Mariotti et al., 2010). A thorough understanding of sediment stability in mudflats is necessary for the management of these delicate environments.

Critical shear stress, the magnitude of shear stress sediments

Corresponding author. E-mail address: sergio@bu.edu (S. Fagherazzi). may withstand before significant erosion occurs, is a key parameter controlling erosion of tidal flats (Andersen et al., 2007). Tidal flat sediments are subject to varying shear stresses over tidal cycles due to water currents (Fagherazzi and Mariotti, 2012) and propagation of wind waves (Mariotti and Fagherazzi, 2012a). Sediments with higher critical shear stress are less susceptible to erosion and therefore are able to withstand higher levels of shear stress before sediment resuspension occurs.

Numerous studies have shown that the erosion threshold of cohesive sediments in muddy tidal flats is controlled by a complex combination of physical, chemical, and biological factors (e.g. Black et al., 2002; Defew et al., 2002; Perillo et al., 2005; Marani et al., 2007). Site-specific properties, such as sediment characteristics (density, organic content, grain size) as well as the presence or absence of microfauna, submerged vegetation, and biofilms make the key mechanisms responsible for sediment stability difficult to discern (Defew et al., 2002).

Mudflats are often colonized by biofilms, of which microphytobenthos (a photosynthetic diatom-dominated assemblage of unicellular, eukaryotic organisms) is a major component (MacIntyre et al., 1996). Among other factors, microphytobenthos growth is susceptible to light, temperature, and nutrient availability, leading to seasonal changes in their abundance (Davoult et al.,

2009). Microphytobenthos produce an extracellular carbohydrate matrix that may contribute to sediment stabilization (e.g. de Brouwer et al., 2002; Tolhurst et al., 2003; de Brouwer et al., 2005; Mariotti and Fagherazzi, 2012b). Previous research has found a positive correlation between biofilm biomass and erosion threshold in tidal flat sediments (Underwood and Paterson, 1993; Black et al., 2002; Tolhurst et al., 2003). The relationship between biofilm presence and increased sediment stability is thought to be due to sediment binding and a decrease in roughness and drag on the sediment surface (Tolhurst et al., 2008a,b). The role microphytobenthos play in sediment stability may vary throughout the tidal cycle due to their migration within the sediment (e.g. Paterson, 1989; Miller et al., 1996; Defew et al., 2002).

Studies of tidal mudflats have indicated that the erosion threshold varies over emersion-submergence cycles and depends on the environmental conditions sediments are exposed to (Amos et al., 1988). Erosion threshold has been shown to increase over tidal emersion periods, but returns to its pre-exposure value once exposed to tidal submergence (Tolhurst et al., 2006a). Moreover, rainfall directly falling over a subaerial tidal flat during low tide can increase resuspension (Chen et al., 2015).

The physical properties of clay soils, which dominate tidal mudflats, can vary significantly with the degree of hydration (Hillel, 1998). The shear strength increases as the soil de-saturates and the matric soil potential increases (Zhan and Ng, 2006).

Similarly, seasonal and climatic factors have a great influence on sediment erodibility when measured over long time periods (Amos et al., 1988). While temporal changes in sediment erosion threshold have been studied both seasonally and over single tidal cycles, changes resulting from variations in daily environmental conditions have yet to be considered.

Here we present results on a field experiment conducted on a tidal flat in Plum Island Sound, Massachusetts, in September 2011. This study explores the connections between critical shear stress, biofilm abundance, and evaporation. Field observations taken during emersion were used to identify biological and physical factors contributing to changes in erosion threshold of tidal flat sediments.

### 2. Study site

The study took place along the Rowley River Estuary in Rowley, Massachusetts, within the Plum Island Sound Long Term Ecological Research site (Fig. 1). The Rowley River forms at the convergence of the Egypt River and Muddy Run in Ipswich, and covers a drainage

area of 9.6 square miles. The Rowley River flows into Plum Island Sound, a semi-diurnal estuary connected to the Gulf of Maine that experiences a mean tidal range of 2.6 m and spring tidal range of 3.2 m. Tidal flats consisting primarily of muddy sediments become subaerial along the banks of the Rowley River during low tide. Previous research in this area has found that these environments support a large population of benthic, pennate diatoms (Tobias et al., 2003) that are more common in sandy areas within the Sound (Fagherazzi et al., 2014).

#### 3. Materials and methods

A two-week study into the daily variability in the erosion threshold of tidal flat sediments was conducted in September 2011. Field observations were used to investigate how changes in environmental conditions impact the erosion threshold of tidal flat sediments during emersion. Additionally, hydrological and meteorological sensors located in proximity of the study site were used to model the hydrodynamic processes occurring during submergence. This approach was used to determine whether sediment resuspension during submergence was related to meteorological conditions during the previous emersion period.

A rectangular transect 6 m by one was established on a mudflat near the Rowley river. The transect, divided in six  $1 \times 1$ m squared plots, stretched from the salt marsh scarp to the channel (Fig. 1). The total change in elevation along the transect was less than 0.4 m. High-resolution measurements of critical shear stress, chlorophyll a concentration, dry density, and organic content were taken daily. An acoustic Doppler velocimeter (ADV) was deployed 3 m upstream to monitor hydrological conditions (Fig. 1). A meteorological station located approximately 2.9 miles from the study site was used to monitor weather conditions during the experiment. A detailed description of the instruments and methods used in this research is reported below.

## 3.1. Erosion threshold

The erosion threshold of each plot was measured daily using a Cohesive Strength Meter, CSM (Widdows et al., 2007; Tolhurst et al., 1999). CSM measurements were taken only when the study site was subaerial. The CSM provides a relative erosion threshold for comparing measurements at different locations. It measures the erosion threshold of sediments by shooting a vertical jet of water with increasing force into a chamber applied on the sediment substrate. This device allows for repeated measurements taken

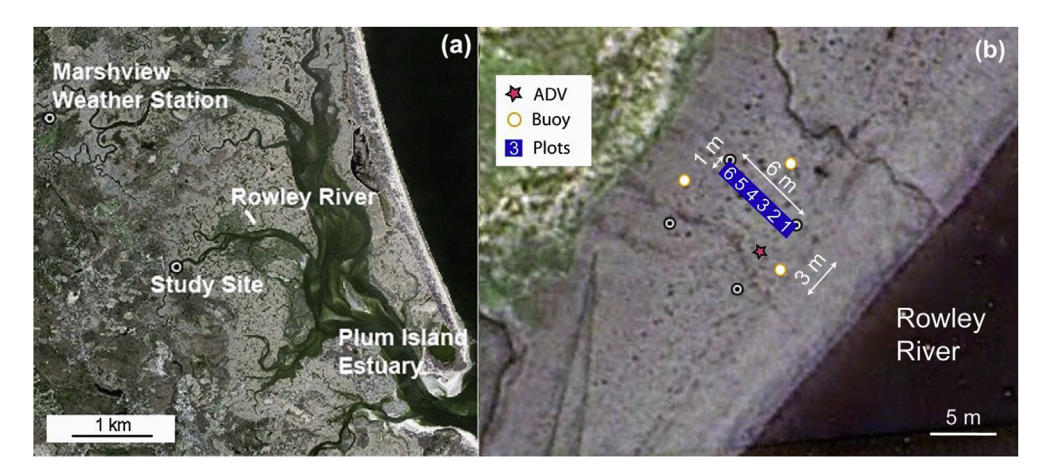


Fig. 1. (a) Map of Plum Island Estuary including study site and Marshview weather station. (b) Map of study site transect and ADV location during the measurements. Image courtesy of Google Earth, Imagery Date (a) 04/17/2008, (b) 06/18/2012.

over a short time period and a small area, making it ideal for studying spatial and temporal variability within a single field site (Tolhurst et al., 2006b). An infrared sensor monitors the turbidity levels within the chamber to determine the pressure of the jet at which significant erosion begins. The erosion threshold was determined as a change in the slope in the plot relating jet strength exerted by the CSM and turbidity measured within the chamber (Tolhurst et al., 1999).

The jet pressure of the CSM was converted to stagnation pressure on the sediment surface using the calibration equations reported in Vardy et al. (2007). The stagnation pressure is a measure of the sediment stability and it was linearly related to the critical shear stress for erosion by Grabowski et al. (2010). However, this calibration was carried out for soft, fluvial sediments with a high fraction of sand and cannot be directly applied to our site that is characterized by a muddy substrate. Since an exhaustive calibration of the instrument is not available, we will report the results in terms of stagnation pressure, as suggested by Vardy et al. (2007). A similar methodology has been adopted by Spears et al. (2008). Note that even if the CSM cannot directly measure the critical shear stress for erosion, it can be used to detect differences in relative erosion threshold in time and space, and as such it has been widely used by researchers in the recent past (e.g. Spears et al., 2008; Grabowski et al., 2012; Chen et al., 2012).

Three erosion threshold measurements were taken each day. Measurements were taken randomly within plots, starting from the lower plot and ending with the higher plot and alternating between even and odd plots daily. Each measurement took approximately 20 min.

#### 3.2. Bottom velocities and shear stresses

Hydrodynamic conditions on the tidal flat were monitored with a Nortek Acoustic Doppler velocimeter (ADV) deployed 3 m away from the transect from September 6, 2011 at 12:00 to September 29, 2011 at 00:00 (Fig. 1). The ADV was deployed near plot 1 at an elevation of -1.032 m relative to mean sea level (Fig. 1). The shear stress exerted on the tidal flat during each tidal cycle was calculated from the high frequency velocity measurements of the ADV using the Reynolds stress method (Andersen et al., 2007).

In addition to the critical shear stress, the rate of sediment resuspension and related fluxes occurring over tidal cycles is critical for a complete understanding of sediment erodibility (Amos et al., 1992). Here we assume that the sediment concentration measured at this location is a proxy for sediment resuspended in a larger part of the sound and funneled in the river during flood. Similarly, the shear stresses measured at this location are a proxy for the shear stresses exerted in other tidal flats downstream in the river and sound and, more generally, a proxy for tidal forces acting on surfaces at similar elevations. We chose the maximum sediment concentration during flood as a proxy of sediment resuspended and advected from the sound in the river, and the maximum shear stress during flood as a proxy of tidal forces.

Backscatter intensity recorded by the ADV was used herein as a proxy for suspended sediment concentration (Ha et al., 2009; Chanson et al., 2008). The backscatter signal is generated from sound pulses reflecting off particles suspended in the water column. Measuring the suspended sediment concentration with an ADV allows for water velocity and shear stress measurements to be taken in conjunction. The maximum backscatter recorded by the ADV during each tidal cycle was used as an indicator of sediment resuspension in the sound and it is compared to the total evaporation from the preceding emersion cycle. Backscatter for each ADV measurement is calculated as the average of the signal/noise for the x, y and z components. The backscatter signal was calibrated in the

laboratory with sediment collected at the field location (Fig. 2).

Sediments were collected in the first centimeter of the tidal flat bottom and mixed in a tank with water taken at the site to produce different suspended sediment concentrations (SSC). The ADV backscatter was measured for each sediment concentration in the tank. A linear fit between ADV backscatter in dB and the logarithm of the sediment concentration yielded a correlation coefficient  $R^2 = 0.92$ , p < 0.05 (Fig. 2, see also Fugate and Friedrichs, 2002). The maximum backscatter during flood occurs generally 1–1.5 h after tidal flat submergence (Fig. 3).

#### 3.3. Emersion period and variations in bed elevation

The ADV pressure sensor was used to determine when the tidal flat was subaerial submerged during each tidal cycle. The time of exposure and submergence were determined by fitting a polynomial on the pressure data and then extrapolating the time equivalent to a zero pressure. This value was used to calculate the length of time the tidal flat was subaerial prior to the measurement of the critical shear stress.

Changes in mudflat elevation were determined using the ADV acoustic ping measurements. The ADV was firmly mounted on auger frames and remained at a constant elevation throughout the experiment. An acoustic ping measured the distance from the instrument to the bed surface at the beginning and end of each measurement period. The net variation in bottom elevation during each tidal cycle was calculated as the difference between the maximum distance from the ADV (which represents the maximum erosion) and the final distance before exposure. Both the bed elevation and effective deposition during the previous submergence period were considered as possible factors affecting daily changes in critical shear stress.

# 3.4. Chlorophyll a

Duplicate subcores were taken in each of the six experimental plots on alternate days for analysis of chlorophyll a. The subcores were 1 cm in diameter and sampled the top 1 cm of tidal flat sediment. Each was divided into 0.5 cm increments and frozen until analysis. For sediment chlorophyll a concentration analysis, sediment subcore sections were thawed, sonicated, and extracted in

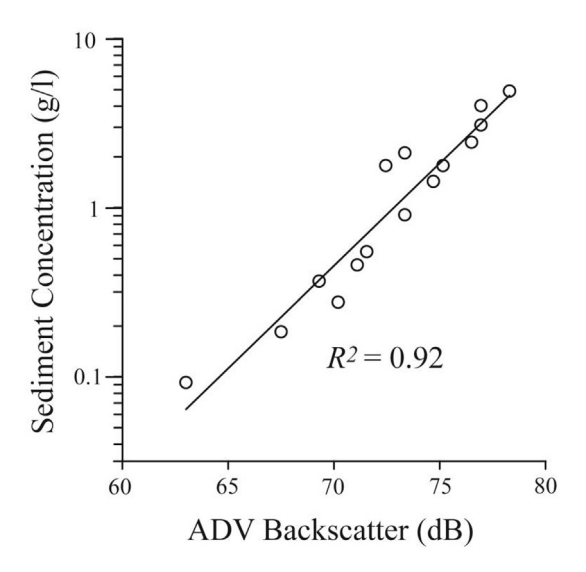


**Fig. 2.** Calibration of the ADV backscatter signal with suspended sediment concentrations measured in the laboratory using in situ surficial sediments.

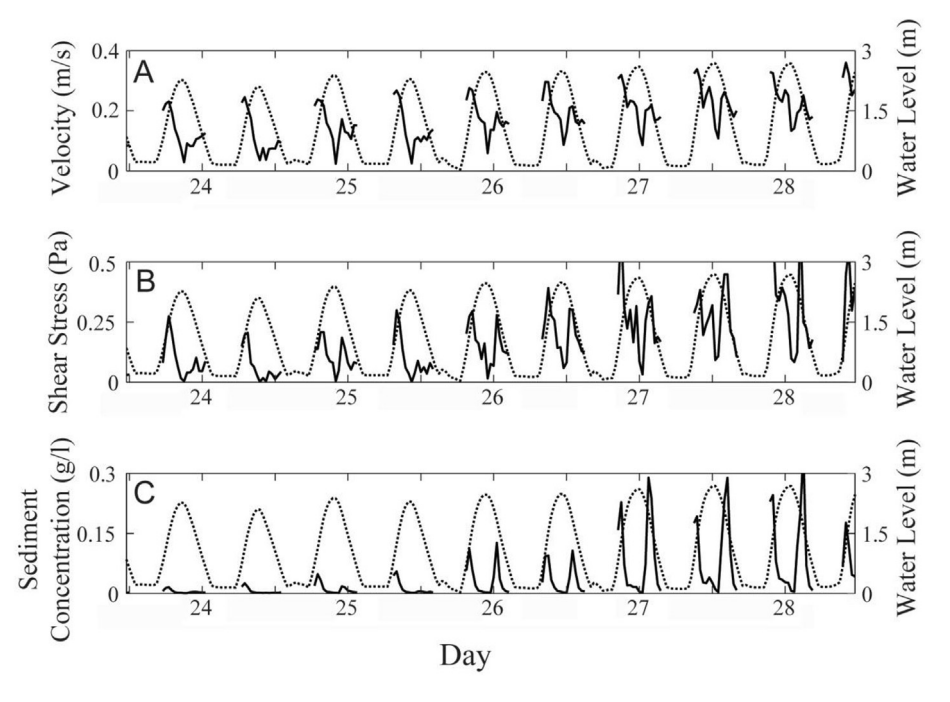


Fig. 3. A) absolute velocity, B) bottom shear stress, C) Sediment concentration as a function of time from 9/23/2011 to 9/28/2011. The dotted lines in all three graphs represent water levels (value zero when the flat is subaerial).

90% acetone overnight (Dalsgaard, 2000). Extracted samples were then centrifuged and 2 mL aliquots were analyzed for chlorophyll *a* fluorescence on a Turner Trilogy Fluorometer.

#### 3.5. Sediment characteristics

Syringe core samples were used to monitor changes in the density and organic content of each plot. A 15 cc sediment sample was taken each day in conjunction with the erosion threshold measurements. The samples were dried in an oven at 60 °C, and weighed to determine dry density. The samples were pulverized with a mortar and pestle, weighed and put into an oven at 500 °C for 18 h, and re-weighed to determine the percent organic material in the sample. Soil temperature was measured once per day before the CSM measurement using a Decagon 5 TM Water and Temperature Probe and ProCheck Handheld reader.

A 50 cc sample was taken from each plot on the first and last days of field observations. The samples were sieved to determine the percent of sand and silt/clay present at the study site and determine any variations in grain size of the sand across the transect. The median grain size of sand was determined using the geometric method of moments in GRADISTATV8 (Blott and Pye, 2001).

#### 3.6. Meteorological conditions

A weather station run by the Marine Biological Laboratory (MBL) at Marshview Field Station was used to monitor daily meteorological conditions (Fig. 1). All data were collected using a Campbell Scientific CR10X data logger and averaged for 15 min. Air temperature and relative humidity were measured using a Vaisala HPM45C. Wind speed was measured using a RM Young 05103. Precipitation was recorded using Texas Electronic TE525WS-L. Solar radiation was measured using a Licor LI200X-L pyranometer. All

sensors were mounted 3.048 m (10 feet) above ground level. The weather station is located in a more sheltered area with respect to the Rowley River, with sparse trees possibly reducing wind speed. Therefore wind speed could be quite different at the site.

# 3.7. Evaporation rates

Changes in daily meteorological conditions affect the rate of evaporation and therefore the soil characteristics of tidal flat sediments. The evaporation rate was calculated using the temperature of the sediments collected together with the erosion threshold and weather data at the time of tidal flat emersion. The evaporation rate was calculated using the mass transfer approach when the sediment temperature was available (i.e. tidal cycles when the erosion threshold was measured). The evaporation E reads (Dingman, 1994):

$$E = K_E \nu_a (e_{soil} - e_{air}) \tag{1}$$

where  $K_E$  is the efficiency of vertical water vapor transport,  $v_a$  is wind speed, and  $e_{soil}$  and  $e_{air}$  are the vapor pressures of the soil surface and air respectively.  $K_E$  is calculated as (Dingman, 1994):

$$K_E = \frac{D_{WV}}{D_M} \frac{0.622 \rho_a}{P \rho_w} \frac{1}{6.25 \ln \left[ \left( \frac{z_m - z_d}{z_0} \right) \right]^2}$$
 (2)

where  $D_{WV}$  is the diffusivity of water vapor,  $D_M$  is the diffusivity of momentum,  $z_o$  is the roughness height,  $z_d$  is the zero-plane displacement,  $z_m$  is the elevation at which wind speed is measured, P is the atmospheric pressure,  $\rho_a$  and  $\rho_w$  the densities of air and water respectively.

The vapor pressure of air and soil are (Dingman, 1994):

$$e_{air} = 6.11 W_a \exp\left(\frac{17.3T_{air}}{T_{air} + 237.2}\right); \quad e_{soil}$$
  
=  $6.11 \exp\left(\frac{17.3T_{soil}}{T_{soil} + 237.2}\right)$  (3)

where  $W_a$  is the relative humidity,  $T_{air}$  and  $T_{soil}$  are the temperature of the air and soil in  ${}^{\circ}$ C.

Penman's equation was used to estimate the evaporation rate when soil temperature data were absent (i.e. when erosion threshold measurements were not taken). According to this equation, the rate of evaporation is calculated as (Dingman, 1994):

$$E = \frac{s(T_{air})(K+L) + r\rho\lambda_{v}K_{E}\nu_{a}e_{sat}(T_{air})(1-W_{a})}{\rho\lambda_{v}(s(T_{air}) + r)}$$
(4)

where K is solar radiation, L is net long wave radiation,  $v_a$  is wind speed,  $\Upsilon$  is the psychometric constant,  $K_E$  is the efficiency of vertical water vapor transport,  $\lambda_V$  is the latent heat of vaporization,  $s(T_{air})$  is the slope of saturation vapor pressure curve and  $e_{sat}(T_{air})$  is the vapor pressure of air at saturation.  $K_E$  is calculated using Eq. (2). Published constant values were used for the latent heat of vaporization (2257 kJ/kg), the psychometric constant (0.66 mbar/C) and density of water (1000 kg/m³).  $s(T_{air})$  and  $e_{sat}(T_{air})$  are calculated as (Dingman, 1994):

$$s(T_{air}) = \frac{25083}{(T_{air} + 237.3)^2} \exp\left(\frac{17.3 T_{air}}{T_{air} + 237.3}\right)$$
 (5)

$$e_{sat}(T_{air}) = 6.11 \exp\left(\frac{17.3T_{air}}{T_{air} + 237.3}\right)$$
 (6)

Net long wave radiation, L, is calculated as the difference between incoming atmospheric radiation,  $L_{at}$ , and radiation emitted by the sediment surface,  $L_w$ , (Abramowitz et al., 2012; Dingman, 1994):

$$L = L_{at} - L_{w}$$

$$L_{at} = (031e_{air} + 2.84 T_{air} - 522.5)*.001$$

$$L_{w} = \varepsilon_{w}O'(T_{air} + 273.15)^{4}$$
(7)

Published constant values were used for the emissivity of water,  $\epsilon_w$  (0.97) and the Stefan-Boltzmann constant O′ (5.67  $\times$   $10^{-11}$  kW/  $m^2 K^4$ ).

In order to calculate the efficiency of vertical water vapor transport,  $K_E$ , an acceptable roughness height,  $z_0$ , had to be determined for the study site. This was computed by comparing the rate of evaporation calculated with the Penman's equation (Eq. (4)) with the rate computed with the mass transfer approach (Eq. (1)). A value of  $z_0 = 0.158$  m was found by minimizing the mean squared error between the results of the two methods.

The evaporation rate was multiplied by the length of exposure to determine the evaporation that occurred prior to the erosion threshold measurement. Exposure time was determined by the ADV pressure data; time of critical shear strength measurements was taken from the CSM measurement timestamp. Total evaporation during emersion was instead defined as evaporation rate times the total period of tidal emersion. Exposure and submergence time were determined by the ADV pressure data, after correcting for atmospheric pressure using the data from the weather station.

#### 3.8. Statistical analysis

A multi-faceted approach was used for the statistical analysis of the field observations component of this study. To test whether bottom sediment characteristics (percent of mud, dry density, and percent of organic matter) changed during the study, differences between measurements taken in the same plot of each transect on different days were tested using a two-way ANOVA. The influence that each measured factor (chlorophyll *a*, sediment characteristics, and meteorological conditions) had on the erosion threshold was determined through a correlation analysis. The combined influence of all variables reporting a significant correlation with erosion threshold was determined through a multiple regression analysis.

The influence the maximum shear stress exerted on tidal flat sediments was analyzed using correlation analysis. Similarly, a correlation analysis determined the influence the total evaporation over emersion periods exerted individually on the maximum sediment concentration measured during the following flood period.

A multiple regression analysis was used to determine how much of the variability seen in the maximum sediment concentration can be accounted for by considering total evaporation and bottom shear stress together. The Cook's distance approach was used to identify outliers (Cook, 1977). We checked whether any data point with a Cook's distance  $D_i > 4/n$ , where n is the number of observations, was influencing the linear regressions.

#### 4. Results

#### 4.1. Sediment characteristics

Sediment characteristics along the transect remained relatively unchanged throughout the experiment. Average dry density fluctuated daily between 900 and 1100 kg/m<sup>3</sup>. Although some fluctuations in the daily dry density were recorded, no trends were found in these fluctuations.

Percent organic material in the plots showed no significant change over the duration of the experiment. The mean percent organic material varied daily from 3 to 4.5%; however, no trend emerged from the data. Finally, little variation without any clear trend in grain size was seen from samples taken at the beginning and end of the experimental period. Samples from each plot at the beginning and end of the experiment showed the sediments were approximately 60–65% clay/silt and 35–40% sand.

### 4.2. Factors controlling substrate critical shear stresses

Erosion threshold was not related to the elevation of each plot with respect to mean sea level ( $R^2=0.09,\,p>0.05$ ). A significant difference was found in the daily erosion threshold measurements taken within the same plots on different days (p<0.05), implying that variations in daily environmental conditions were affecting sediment erodibility within the plots (Fig. 4).

Correlation analysis showed that the length of exposure to air prior to the CSM measurement cannot explain the differences in erosion threshold. In fact, the variability in erosion threshold increased as sediments were subaerial for a longer period of time. When the daily evaporation rate was considered together with the length of exposure (total evaporation), a monotonic trend was detected, with erosion threshold growing as a function of total evaporation (Kendall's  $\tau=0.30$  with p<0.05, Spearman's  $\rho=0.42$  with p<0.05). Moreover a significant linear correlation between the erosion threshold and the square root of the total evaporation was found ( $R^2=0.36$ , p<0.05, statistical power  $\pi=0.95$ ) (Fig. 5A).

A negative linear relationship was present between chlorophyll a and the erosion threshold of tidal flat sediments ( $R^2=0.23$ , p<0.05, statistical power  $\pi=0.58$ ) (Fig. 5B), indicating that microphytobenthos were fewer when the sediment was stronger (Kendall's  $\tau=-0.37$  with p<0.05, Spearman's  $\rho=-0.56$  with

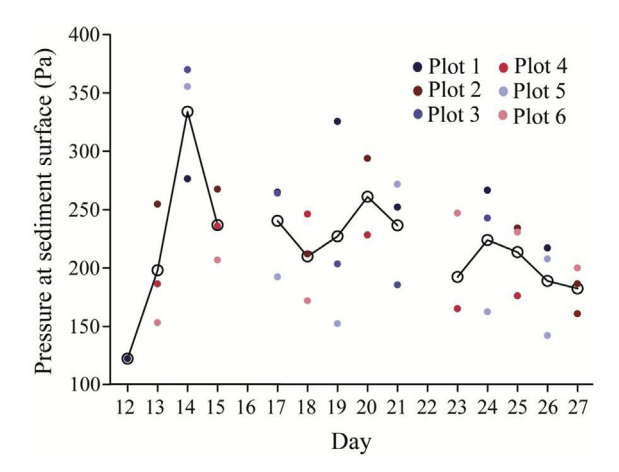


Fig. 4. Erosion threshold in each of day of the experiment. The solid circles are the single measurements while the white circles are the daily averages.

p < 0.05). No statistically significant relationship was found between chlorophyll a concentration and the total evaporation calculated prior to the CSM measurements (p = 0.08, statistical power  $\pi = 0.41$ , Fig. 5C). It should be noted that the time at which chlorophyll a samples were taken was not recorded and we used the time of the CSM measurements as a proxy. As a consequence the relationship between total evaporation and chlorophyll a may be stronger than depicted in this analysis. The erosion threshold of tidal flat sediments was also found to be positively correlated to the average distance between ADV and sediment bed (p = 0.03). The distance from the sediment bed varied during the entire deployment between 28.5 cm and 29.5 cm. The relationships between chlorophyll a and erosion threshold and between chlorophyll a and total evaporation might be affected by the limited number of data points and by the depth of the sediment cores used for the analysis. Chlorophyll a is usually concentrated in the top 2 mm, so a 5 mm deep core might dilute the Chlorophyll a measurement and weaken the relationships with other variables (e.g., Kelly et al., 2001).

A multiple regression analysis was used to determine which significant variables from the correlation analysis were collectively contributing to changes in the observed erosion threshold of the tidal flat sediments. Average change in bottom elevation was not significant when combined with total evaporation in a multiple regression analysis. Similarly, total evaporation and chlorophyll a were not significantly correlated with erosion threshold when considered together in a multiple regression analysis.

#### 4.3. Factors affecting water turbidity on the Rowley River tidal flats

Acoustic backscatter recorded by the ADV during the flood period was used as a proxy for sediment resuspension occurring on the tidal flat as well as for sediments remobilized in several tidal flats within Plum Island Sound and then funneled in the Rowley River.

The sediment concentration recorded by the ADV appears to grow with maximum shear stress exerted locally on the tidal flat (Kendall  $\tau = 0.34$  with p < 0.05, Spearman  $\rho = 0.46$  with p < 0.05) and to decrease as a function of total evaporation recorded during the previous tidal cycle (Kendall  $\tau = -0.37$  with p < 0.05, Spearman  $\rho = -0.51$  with p < 0.05). The logarithm of the sediment concentration also linearly correlates with the logarithm of the maximum shear stress ( $R^2 = 0.34$ , p < 0.05, statistical power  $\pi = 0.98$ , Fig. 6A) and the total evaporation during the previous cycle ( $R^2 = 0.28$ , p < 0.05, statistical power  $\pi = 0.87$ , Fig. 6B). A multiple linear

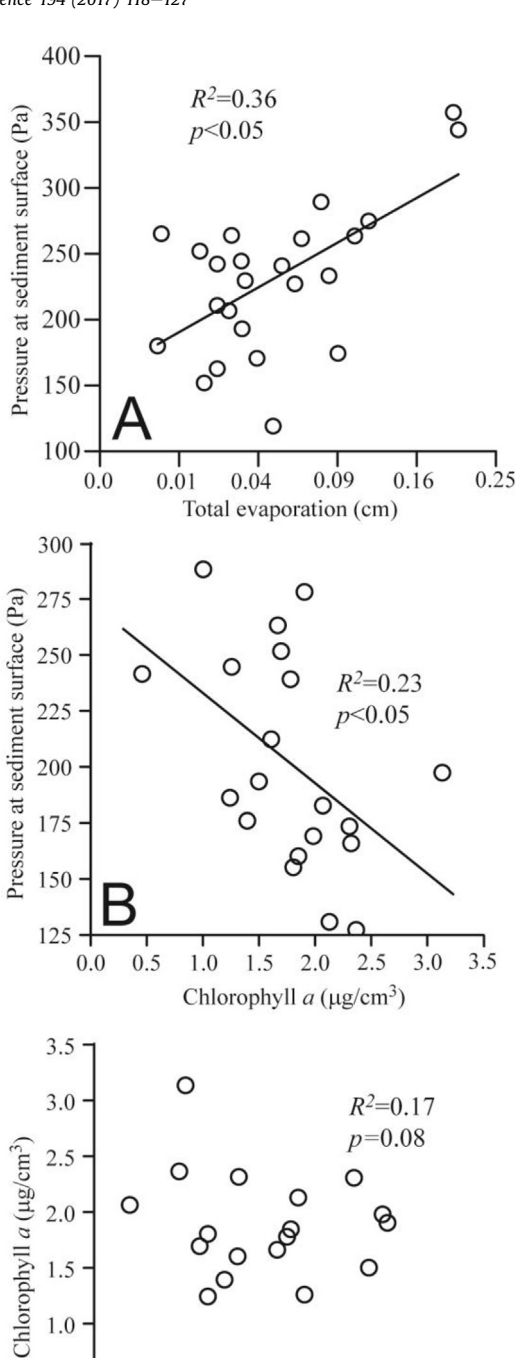


Fig. 5. Relationship between (A) erosion threshold and squared root of total evaporation, (B) erosion threshold and concentration of chlorophyll a, (C) concentration of chlorophyll a and total evaporation.

0.03

Total evaporation (cm)

0.02

1.5

1.0

0.5

0.0

0.0

0.01

0

0.04

0

0.05

regression analysis showed that the total evaporation occurring during the previous tidal cycle and the maximum shear stresses exerted on the tidal flat during flood are independent factors, both controlling the maximum sediment concentration and therefore sediment resuspension. Both factors remain statistically significant when considered together and explained approximately 53% of the

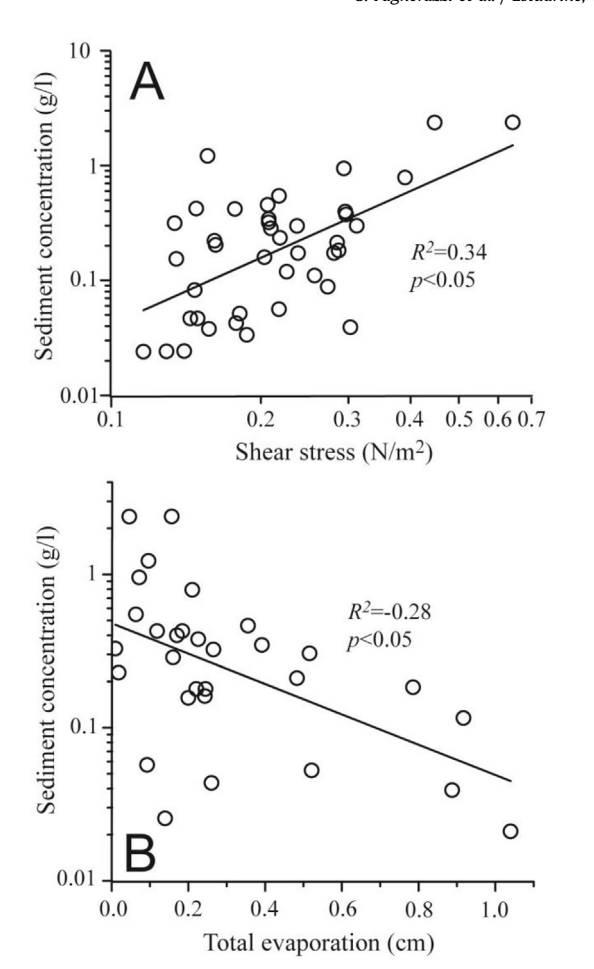


**Fig. 6.** (A) Bottom shear stress versus sediment concentration recorded by the ADV; (B) Evaporation versus sediment concentration recorded by the ADV.

variability in the logarithm of sediment concentration (p < 0.05).

#### 5. Discussion and conclusions

The results of this study show that evaporation is likely associated with daily variations in sediment erodibility of tidal flat sediments. The erosion threshold of the substrate seems to increase as evaporation occurs over the emersion period. The extent of evaporation that tidal flat sediments undergo depends on meteorological conditions (temperature, relative humidity, wind conditions, and solar radiation) as well as the duration of exposure to air. As these conditions change between emersion periods, so does the rate of evaporation and therefore the erosion threshold of the tidal flat sediments. Days with strong winds, warmer temperatures, or more sunlight favor higher evaporation rates. As sediments are subaerial for longer lengths of time, these differences become more pronounced, leading to the increased variability in sediment erosion threshold.

In Fig. 5A two points with high evaporation exert a strong influence on the relationship between evaporation and sediment erodibility. For example, significant variations in the average erosion threshold were evident between September 12 and September 15, with a very high peak in evaporation occurring on September 14 (Fig. 4). The rate of evaporation during emersion increased each day from September 12 to September 14 due to progressively earlier sunrises in relation to the tidal cycle and higher air temperature during emersion (Fig. 7). Additionally,

September 14 exhibited high wind speeds and low relative humidity at the beginning of the emersion period, before erosion threshold measurements were taken. Although sunrise occurred earlier in the tidal cycle on September 15 than on September 14, solar radiation was less, air temperature was similar, while wind speed was low and relative humidity high. These conditions led to a decrease in the rate of evaporation and therefore a decrease in the erosion threshold measured on September 15 (Fig. 4). This evidence supports our finding that the erosion threshold of tidal flat sediments varies significantly with meteorological conditions they are exposed to during emersion. Varying meteorological conditions must be considered to correctly interpret changes in critical shear strength in studies spanning multiple days, and particularly across months or seasons.

Previous studies have shown that biofilm abundance, measured using chlorophyll a as a proxy, has a positive effect on the critical shear strength of tidal flat sediments (Underwood and Paterson, 1993; Tolhurst et al., 2008a,b; Defew et al., 2002). On the contrary, our study found a negative relationship between these two variables. It is important to note that this relationship is not very strong, with low coefficient of determination ( $R^2 = 0.23$ ) and low statistical power ( $\pi = 0.58$ ), possibly indicating that many processes are at play and that Chlorophyll a is not a leading driver of erodibility in this data set.

Diatoms, which are dominant in microphytobenthos, are known to migrate into the sediment over the tidal cycle as water content decreases (Consalvey et al., 2004; Coelho et al., 2009). Therefore the decrease in chlorophyll a may be a result of diatom migration due to sediment desiccation rather than a direct effect of biofilms on critical shear stress. However, chlorophyll a was measured within the top 0.5 cm, and it is unlikely that the microphytobenthos migrated so deep in a tidal cycle. Another possible explanation of reduced chlorophyll a concentrations is grazing by periwinkles (Littorina spp.), which are extremely abundant on these tidal flats. Periwinkles might be more active during warm days thus reducing the biofilm stock. In fact periwinkles have been showed to respond to both desiccation of the sediments and temperature (Chapman and Underwood, 1996). Periwinkles could also bioturbate the top sediment layer, possibly increasing erodibility. Biofilm may partially stabilize loose unconsolidated surface sediment; so whilst the effect of the biofilm is still stabilizing, the high water content and loose open structure of the sediment results in a low erosion threshold. This was seen in areas where a diatom biofilm had lower bulk densities and hence lower erosion thresholds (Tolhurst et al., 2008a,b). Also, biofilms may trap oxygen bubbles, resulting in buoyant biofilms with a lower erosion threshold.

The CSM applies a vertical jet rather than a more realistic shear flow to determine the critical shear stress of the sediments. The biofilm mat is likely more resistant to shear forces as opposed to a vertical jet. It is possible that the jet breaks the biofilm mat more easily than it would erode bare sediment, producing a spike in turbidity. The relationship between chlorophyll a concentration and erosion threshold may not be causal but just reflect the relationship found between total evaporation and erosion threshold. More research is clearly needed to determine the possible causes of a negative relationship between chlorophyll a, evaporation, and erosion threshold.

In addition to the total evaporation and chlorophyll *a* measurements, the average elevation of the mudflat during the previous submergence period was significantly correlated to the critical shear stress. Changes in bed height are a result of erosion and deposition that occurred during the previous submergence cycle. A lower elevation implies an erosion event and the re-exhumation of more compact and resistant sediments. A higher elevation indicates a deposition event, with soft sediment accumulated at the surface.

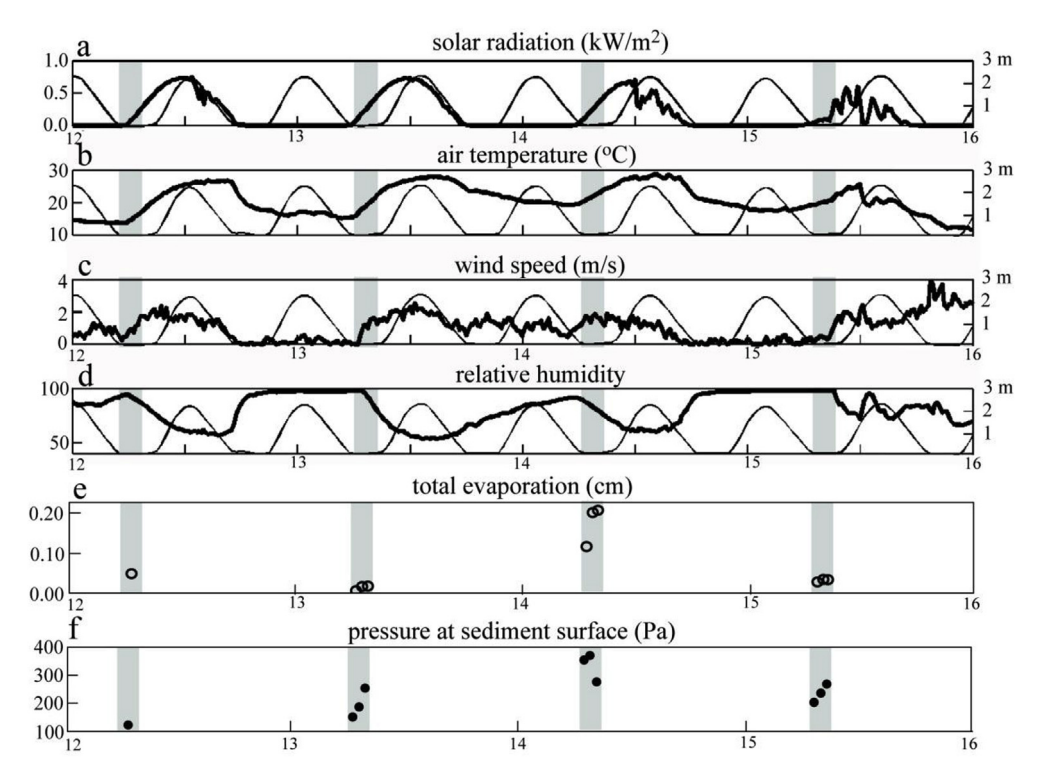


Fig. 7. Meteorological Data from Marshview Field Station from 9/12/2011 to 9/16/2011. A) Solar radiation; B) Air temperature; C) Wind speed; D) Relative humidity; E) Total evaporation; F) erosion threshold of sediments. Gray lines represent corresponding ADV pressure data (water level). Shaded areas represent the time interval between tidal flat exposure and erosion threshold measurement.

Wetting and drying can also alter the bed elevation. As the sediment dries out it compacts, becoming more resistant to erosion. Although changes in the average bed height during the preceding submergence period showed statistical significance with the erosion threshold of sediments, a very low coefficient of determination ( $R^2 = 0.06$ ) indicates that this interaction was limited.

In cohesive sediments, erodibility is related to bulk density and water content (Grabowski et al., 2012). Dense sediments have low erodibility (Amos et al., 2004; Bale et al., 2006, 2007). High water contents, directly affecting plasticity, increase erodibility (Winterwerp and van Kesteren, 2004), Anderson and Howell (1984) indicate that during emersion muddy tidal flats undergo dewatering, because of dessication and drainage. Fiot and Gratiot (2006) studied the structural effect of wetting and drying cycles on tropical mudflats, showing that the sediment beds are subject to compaction, water loss, and a reduction in sediment erodibility when subaerial. Geotechnical measurements in cohesive sediments dredged from coastal areas indicate that dessication reduces water content and void ratio, increasing density (Stark et al., 2005). Dessication therefore triggers dewatering and sediment compaction, decreasing erodibility. Dessication is probably more effective in sediment beds with high water adsorption, like clays with a high fraction of montmorillonite (Grim, 1962) or with high organic content (Keller, 1982). These sediments are more likely to experience a sharp decrease in water content and therefore erodibility during dessication.

It is important to note that tidal flats are subject to erosion and deposition only during submergence periods. Therefore, the importance of our findings from data taken during emersion periods is limited unless the substrate retains its strength after flooding.

The maximum shear stress exerted on the tidal flat by currents occurs during flood, approximately 1–1.5 h after submergence, and

varies with tidal amplitude (larger tides trigger larger shear stresses, Fig. 3). Higher measured shear stresses translate to increased sediment resuspension, leading to a relationship between measured shear stresses and acoustic backscatter (a proxy for sediment concentration) during flood.

The influence of shear stress on the maximum sediment concentration was easily observed towards the end of the study period when spring tides were creating strong flood currents (Fig. 3). In fact, from September 23 to September 28, as the tidal range became larger, the shear stress exerted on the tidal flat sediments increased. Accordingly, sediment concentration grew during this period. However, careful examination shows that current shear stress alone cannot be responsible for all of the variability in sediment concentration among tidal cycles. In fact, the sediment concentration should follow the variations in maximum shear stress between the evening of September 23 and the morning of September 24 and between the two tidal cycles on September 26. In each of these examples, a noticeable increase in the shear stress exerted on the tidal flat sediments does not correspond to an increase in the sediment concentration signal.

Therefore, additional factors must have an influence on sediment concentration in the river during the flood period. For example, wind waves in the sound can resuspend sediments that are then transported in the river and tidal channels during flood (e.g. Fagherazzi and Priestas, 2010). Our study area has very small fetch and therefore waves are not very high. During the study period we measured only two wave events with maximum wave height of 30 cm, on September 6 at 19:30 and on September 17 at 12:00. In both cases we did not detect a significant increase in sediment concentration.

Rainfall can also destabilize and mobilize tidal flat sediments that can be eroded during the following high tide (e.g. Mwamba and Torres, 2002; Tolhurst et al., 2008a, 2008b). During the study

period it rained only twice when the tidal flat was emergent, on September 22 between 0:00 and 2:00 and on September 24 between 0:00 and 3:00. In both cases we did not notice a significant increase in suspended sediment occurring during the next submergence period. The erosion threshold of the tidal flat sediments slightly decreased after both events, measured during the next low tide (Fig. 4).

In addition to the positive correlation with shear stress, the rate of sediment resuspension during flood is negatively related to the amount of evaporation during the previous tidal cycle (Fig. 6B). This finding indicates that changes in erodibility due to evaporation last until the following submergence period. While other sediment properties such as density, organic content, grain size, and fraction of clay and silt, may have a significant effect on substrate strength at varying locations within the estuary, these factors were not found to vary at our site.

The low values of the correlation coefficients indicate that the linear regressions presented here cannot be used to predict sediment concentration and critical shear stress (see Prairie, 1996), but only explain part of the variability of these two variables. Additional factors are clearly affecting sediment dynamics in mesotidal mudflats.

Energetic events in the sound (i.e. storms) and evaporation are not independent processes. Increased cloud cover and rainfall during storms reduce evaporation during low tide. Therefore, a bimodal configuration is likely to exist wherein long periods of fair weather reduce sediment resuspension by the compound effect of dessication and limited hydrodynamic energy. On the other hand, storms lasting for several tidal cycles have a double effect on sediment remobilization, with wet conditions during low tide softening the sediments that are then eroded during high tide.

Evaporation processes are more important in meso and macrotidal environments, where large intertidal areas are subaerial at low tide (e.g. Fagherazzi et al., 2014; Mariotti and Fagherazzi, 2011), such as the study area presented here. Seasonal variability in meteorological conditions should also affect mudflat erosion and sediment resuspension. Summer months might favor desiccation thus reducing erodibility, while cold winter months might increase potential erosion. Global warming might therefore decrease the erodibility of intertidal areas by promoting desiccation during emersion.

#### Acknowledgments

This research was supported by NSF awards OCE-0924287, DEB-1237733 (VCR-LTER program), and OCE-1637630 (PIE-LTER program).

Special thanks to Boston University Marine Program students, particularly Julia Luthringer, Mary Katherine Rogener, and Rachel Schweiker which assisted in data collection for this study.

#### References

- Abramowitz, G., Pouyanné, L., Ajami, H., 2012. On the information content of surface meteorology for downward atmospheric long-wave radiation synthesis. Geophys. Res. Lett. 39 (4).
- Amos, C.L., Van Wagoner, N.A., Daborn, G.R., 1988. The influence of subaerial exposure on the bulk properties of fine-grained intertidal sediment from Minas Basin, Bay of Fundy. Estuarine. Coast. Shelf Sci. 27 (1), 1–13.
- Amos, C.L., Daborn, G.R., Christian, H.A., Atkinson, A., Robertson, A., 1992. In situ erosion measurements on fine-grained sediments from the Bay of Fundy. Mar. Geol. 108 (2), 175–196.
- Amos, C.L., Bergamasco, A., Umgiesser, G., Cappucci, S., Cloutier, D., DeNat, L., Flindt, M., Bonardi, M., Cristante, S., 2004. The stability of tidal flats in Venice Lagoon the results of in-situ measurements using two benthic, annular flumes. J. Mar. Syst. 51, 211–241.
- Andersen, T.J., Fredsoe, J., Pejrup, M., 2007. In situ estimation of erosion and deposition thresholds by Acoustic Doppler Velocimeter (ADV). Estuarine, Coast.

- Shelf Sci. 75 (3), 327-336.
- Anderson, F.E., Howell, B.A., 1984. Dewatering of an unvegetated muddy tidal flat during exposure—desiccation or drainage? Estuaries Coasts 7 (3), 225–232.
- Bale, A.J., Widdows, J., Harris, C.B., Stephens, J.A., 2006. Measurements of the critical erosion threshold of surface sediments along the Tamar Estuary using a miniannular flume. Cont. Shelf Res. 26 (10), 1206–1216.
- Bale, A.J., Stephens, J.A., Harris, C.B., 2007. Critical erosion profiles in macro-tidal estuary sediments: implications for the stability of intertidal mud and the slope of mud banks. Cont. Shelf Res. 27 (18), 2303–2312.
- Black, K.S., Tolhurst, T.J., Paterson, D.M., Hagerthey, S.E., 2002. Working with natural cohesive sediments. J. Hydraulic Eng. 128 (1), 2–8.
- Blott, S.J., Pye, K., 2001. GRADISTAT: a grain size distribution and statistics package for the analysis of unconsolidated sediments. Earth Surf. Process. Landforms 26 (11), 1237—1248.
- Chanson, H., Takeuchi, M., Trevethan, M., 2008. Using turbidity and acoustic backscatter intensity as surrogate measures of suspended sediment concentration in a small subtropical estuary. J. Environ. Manag. 88 (4), 1406–1416. Chapman, M.G., Underwood, A.J., 1996. Influences of tidal conditions, temperature
- Chapman, M.G., Underwood, A.J., 1996. Influences of tidal conditions, temperature and desiccation on patterns of aggregation of the high-shore periwinkle, *Lit-torina unifasciata*, in New South Wales, Australia. J. Exp. Mar. Biol. Ecol. 196 (1), 213–237.
- Chen, Y., Thompson, C.E.L., Collins, M.B., 2012. Saltmarsh creek bank stability: biostabilisation and consolidation with depth. Cont. Shelf Res. 35 (1), 64–74.
- Chen, S., Torres, R., Goni, M.A., 2015. Intertidal zone particulate organic carbon redistribution by low-tide rainfall. Limnol. Oceanogr. 60, 1088–1101. http:// dx.doi.org/10.1002/lno.10077.
- Coelho, H., Vieira, S., Serôdio, J., 2009. Effects of desiccation on the photosynthetic activity of intertidal microphytobenthos biofilms as studied by optical methods. J. Exp. Mar. Biol. Ecol. 381 (2), 98–104.
- Consalvey, M., Paterson, D.M., Underwood, G.J., 2004. The ups and downs of life in a benthic biofilm: migration of benthic diatoms. Diatom Res. 19 (2), 181–202.
- Cook, R.D., 1977. Detection of influential observation in linear regression. Technometrics 19 (1), 15–18.
- Dalsgaard, T., 2000. In: Nielsen, L.P., Brotas, V., Viaroli, P., Underwood, G., Nedwell, D.B., Sundbäck, K., Rysgaard, S., Miles, A., Bartoli, M., Dong, L., Thornton, D.C.O., Ottosen, L.D.M., Castaldelli, G., Risgaard-Petersen, N. (Eds.), Protocol Handbook for NICE Nitrogen Cycling in Estuaries: a Project under the EU Research Programme. Marine Science and Technology (MAST III). National Environmental Research Institute, Silkeborg, Denmark, 62 pp.
- Davoult, D., Migné, A., Créach, A., Gévaert, F., Hubas, C., Spilmont, N., Boucher, G., 2009. Spatio-temporal variability of intertidal benthic primary production and respiration in the western part of the Mont Saint-Michel Bay (Western English Channel, France). Hydrobiologia 620 (1), 163–172.
- de Brouwer, J.F.C., Wolfstein, K., Stal, L.J., 2002. Physical characterization and diel dynamics of different fractions of extracellular polysaccharides in an axenic culture of a benthic diatom. Eur. J. Phycol. 37 (1), 37–44.
- de Brouwer, J.D., Wolfstein, K., Ruddy, G.K., Jones, T.E.R., Stal, L.J., 2005. Biogenic stabilization of intertidal sediments: the importance of extracellular polymeric substances produced by benthic diatoms. Microb. Ecol. 49 (4), 501–512.
- Defew, E.C., Tolhurst, T.J., Paterson, D.M., 2002. Site-specific features influence sediment stability of intertidal flats. Hydrology Earth Syst. Sci. Discuss. 6 (6), 971–982.
- Dingman, S.L., 1994. Physical Hydrology. Prentice Hall, New Jersey, 575 pp
- Fagherazzi, S., Priestas, A.M., 2010. Sediments and water fluxes in a muddy coastline: interplay between waves and tidal channel hydrodynamics. Earth Surf. Process. Landforms 35 (3), 284–293.
- Fagherazzi, S., Mariotti, G., 2012. Mudflat runnels: evidence and importance of very shallow flows in intertidal morphodynamics. Geophys. Res. Lett. 39 (14), L14402.
- Fagherazzi, S., Mariotti, G., Banks, A.T., Morgan, E.J., Fulweiler, R.W., 2014. The relationships among hydrodynamics, sediment distribution, and chlorophyll in a mesotidal estuary. Estuarine, Coast. Shelf Sci. 144, 54–64.
- Fiot, J., Gratiot, N., 2006. Structural effects of tidal exposures on mudflats along the French Guiana coast. Mar. Geol. 228 (1), 25–37.
- Fugate, D.C., Friedrichs, C.T., 2002. Determining concentration and fall velocity of estuarine particle populations using ADV, OBS and LISST. Cont. Shelf Res. 22 (11), 1867—1886.
- Galbraith, H., Jones, R., Park, R., Clough, J., Herrod-Julius, S., Harrington, B., Page, G., 2002. Global climate change and sea level rise: potential losses of intertidal habitat for shorebirds. Waterbirds 25 (2), 173–183.
- Grabowski, R.C., Droppo, I.G., Wharton, G., 2010. Estimation of critical shear stress from cohesive strength meter-derived erosion thresholds. Limnol. Oceanogr. 8, 678–685. http://dx.doi.org/10.4319/lom.2010.8.
- Grabowski, R.C., Wharton, G., Davies, G.R., Droppo, I.G., 2012. Spatial and temporal variations in the erosion threshold of fine riverbed sediments. J. Soils Sediments 12 (7), 1174–1188. http://dx.doi.org/10.1007/s11368-012-0534-9.
- Grim, R., 1962. Applied Clay Mineralogy. McGraw-Hill, New York, 430pp.
- Ha, H.K., Hsu, W.Y., Maa, J.Y., Shao, Y.Y., Holland, C.W., 2009. Using ADV backscatter strength for measuring suspended cohesive sediment concentration. Cont. Shelf Res. 29 (10), 1310–1316.
- Hillel, D., 1998. Environmental Soil Physics: Fundamentals, Applications, and Environmental Considerations. Academic press, San Diego CA, 771 pp.
- Keller, G.H., 1982. Organic matter and the geotechnical properties of submarine sediments. Geo-Marine Lett. 2 (3), 191–198.
- Kelly, J.A., Honeywill, C., Paterson, D.M., 2001. Microscale analysis of chlorophyll-a

- in cohesive, intertidal sediments: the implications of microphytobenthos distribution. J. Mar. Biol. Assoc. U. K. 81 (1), 151–162.
- Little, C., 2000. The Biology of Soft Shores and Estuaries. Oxford University Press, Oxford UK, 264 pp.
- MacIntyre, H.L., Geider, R.J., Miller, D.C., 1996. Microphytobenthos: the ecological role of the "secret garden" of unvegetated, shallow-water marine habitats. I. Distribution, abundance and primary production. Estuaries 19 (2), 186–201.
- Marani, M., D'Alpaos, A., Lanzoni, S., Carniello, L., Rinaldo, A., 2007. Biologicallycontrolled multiple equilibria of tidal landforms and the fate of the Venice Res. Lett. 34, L11402. http://dx.doi.org/10.1029/ lagoon. Geophys. 2007GL030178.
- Mariotti, G., Fagherazzi, S., Wiberg, P.L., McGlathery, K.J., Carniello, L., Defina, A., 2010. Influence of storm surges and sea level on shallow tidal basin erosive processes, I. Geophys, Res. 115 (C11), C11012.
- Mariotti, G., Fagherazzi, S., 2011. Asymmetric fluxes of water and sediments in a mesotidal mudflat channel. Cont. Shelf Res. 31 (1), 23-36.
- Mariotti, G., Fagherazzi, S., 2012a. Wind waves on a mudflat: the influence of fetch and depth on bed shear stresses. Cont. Shelf Res. S99–S110, 10.1016/ j.csr.2012.03.001http://dx.doi.org/10.1016/j.csr.2012.03.001.
- Mariotti, G., Fagherazzi, S., 2012b. Modeling the effect of tides and waves on benthic
- biofilms. J. Geophys. Res. 117, G04010. http://dx.doi.org/10.1029/2012JG002064. Meire, P., Ysebaert, T., Damme, S.V., Bergh, E.V.D., Maris, T., Struyf, E., 2005. The Scheldt estuary: a description of a changing ecosystem. Hydrobiologia 540 (1),
- Miller, D.C., Geider, R.J., MacIntyre, H.L., 1996. Microphytobenthos: the ecological role of the "secret garden" of unvegetated, shallow-water marine habitats, II. Role in sediment stability and shallow-water food webs, Estuaries Coasts 19 (2). 202-212
- Mwamba, M.J., Torres, R., 2002. Rainfall effects on marsh sediment redistribution, North Inlet, South Carolina, USA. Mar. Geol. 189 (3), 267-287.
- Paterson, D.M., 1989. Short-term changes in the erodibility of intertidal cohesive sediments related to the migratory behavior of epipelic diatoms. Limnol. Oceanogr. 34 (1), 223-234.
- Perillo, G., Minkoff, D., Piccolo, M., 2005. Novel mechanism of stream formation in coastal wetlands by crab-fish-groundwater interaction. Geo-Marine Lett. 25, 214-220. http://dx.doi.org/10.1007/s00367-005-0209-2.
- Prairie, Y.T., 1996. Evaluating the predictive power of regression models. Can. J. Fish. Aquatic Sci. 53 (3), 490-492.
- Scavia, D., Field, J.C., Boesch, D.F., Buddemeier, R.W., Burkett, V., Cayan, D.R., Titus, J.G., 2002. Climate change impacts on US coastal and marine ecosystems. Estuaries Coasts 25 (2), 149-164.
- Spears, B.M., Saunders, J.E., Davidson, I., Paterson, D.M., 2008. Microalgal sediment biostabilisation along a salinity gradient in the Eden Estuary, Scotland: unravelling a paradox. Mar. Freshw. Res. 59 (4), 313-321. http://dx.doi.org/10.1071/

- MF07164.
- Stark, T.D., Choi, H., Schroeder, P.R., 2005. Settlement of dredged and contaminated material placement areas. II: primary consolidation, secondary compression, and desiccation of dredged fill input parameters. J. Waterw. port, Coast. ocean Eng. 131 (2), 52-61.
- Tobias, C., Giblin, A., McClelland, J., Tucker, J., Peterson, B., 2003. Sediment DIN fluxes and preferential recycling of benthic microalgal nitrogen in a shallow macrotidal estuary. Mar. Ecol. Prog. Ser. 257, 25–36.
- Tolhurst, T.I., Black, K.S., Shavler, S.A., Mather, S., Black, I., Baker, K., Paterson, D.M., 1999. Measuring the in situ erosion shear stress of intertidal sediments with the Cohesive Strength Meter (CSM). Estuarine, Coast. Shelf Sci. 49 (2), 281–294.
- Tolhurst, T.J., Jesus, B., Brotas, V., Paterson, D.M., 2003. Diatom migration and sediment armouring - an example from the Tagus Estuary, Portugal. Hydrobiologia 503 (1), 183–193.
- Tolhurst, T.J., Defew, E.C., Perkins, R.G., Sharples, A., Paterson, D.M., 2006a. The effects of tidally-driven temporal variation on measuring intertidal cohesive sediment erosion threshold. Aquat. Ecol. 40 (4), 521–531.
- Tolhurst, T.J., Defew, E.C., De Brouwer, J.F.C., Wolfstein, K., Stal, L.J., Paterson, D.M., 2006b. Small-scale temporal and spatial variability in the erosion threshold and properties of cohesive intertidal sediments. Cont. Shelf Res. 26 (3), 351–362.
- Tolhurst, T.J., Consalvey, M., Paterson, D.M., 2008a. Changes in cohesive sediment properties associated with the growth of a diatom biofilm. Hydrobiologia 596 (1), 225–239.
- Tolhurst, T.J., Watts, C.W., Vardy, S., Saunders, J.E., Consalvey, M.C., Paterson, D.M., 2008b. The effects of simulated rain on the erosion threshold and biogeochemical properties of intertidal sediments. Cont. Shelf Res. 28, 1217–1230.
- Underwood, G.J., Paterson, D.M., 1993. Seasonal changes in diatom biomass, sediment stability and biogenic stabilization in the Severn Estuary. J. Mar. Biol. Assoc. U. K. 73 (4), 871-887.
- Van Damme, S., Struyf, E., Maris, T., Ysebaert, T., Dehairs, F., Tackx, M., Heip, C., Meire, P., 2005. Spatial and temporal patterns of water quality along the estuarine salinity gradient of the Scheldt estuary (Belgium and The Netherlands): results of an integrated monitoring approach. Hydrobiologia 540 (1), 29-45.
- Vardy, S., Saunders, J.E., Tolhurst, T.J., Davies, P.A., Paterson, D.M., 2007. Calibration of the high-pressure cohesive strength meter (CSM). Cont. Shelf Res. 27, 1190\_1199
- Widdows, J., Friend, P.L., Bale, A.J., Brinsley, M.D., Pope, N.D., Thompson, C.E.L., 2007. Inter-comparison between five devices for determining erodibility of intertidal sediments. Cont. shelf Res. 27 (8), 1174-1189.
- Winterwerp, J.C., van Kesteren, W.G.M., 2004. Introduction to the Physics of Cohesive Sediment in the Marine Environment. Elsevier, Amsterdam, 576pp.
- Zhan, T.L., Ng, C.W., 2006. Shear strength characteristics of an unsaturated expansive clay. Can. Geotechnical J. 43 (7), 751-763.